Int J CARS
DOI 10.1007/s11548-013-0918-3

ORIGINAL ARTICLE

C-arm angle measurement with accelerometer for brachytherapy: an accuracy study

Thomas Wolff · Andras Lasso · Markus Eblenkamp · Erich Wintermantel · Gabor Fichtinger

Received: 10 January 2013 / Accepted: 18 June 2013

Abstract
Purpose X-ray fluoroscopy guidance is frequently used in medical interventions. Image-guided interventional procedures that employ localization for registration require accurate information about the C-arm's rotation angle that provides the data externally in real time. Optical, electromagnetic, and image-based pose tracking systems have limited convenience and accuracy. An alternative method to recover C-arm orientation was developed using an accelerometer as tilt sensor.
Methods The fluoroscopic C-arm's orientation was estimated using a tri-axial acceleration sensor mounted on the X-ray detector as a tilt sensor. When the C-arm is stationary, the measured acceleration direction corresponds to the gravitational force direction. The accelerometer was calibrated with respect to the C-arm's rotation along its two axes, using a high-accuracy optical tracker as a reference. The scaling and offset error of the sensor was compensated using polynomial fitting. The system was evaluated on a GE OEC 9800 C-arm. Results obtained by accelerometer, built-in sensor, and image-based tracking were compared, using optical tracking as ground truth data.
Results The accelerometer-based orientation measurement error for primary angle rotation was $-0.1 \pm 0.0°$ and for secondary angle rotation it was $0.1 \pm 0.0°$. The built-in sensor orientation measurement error for primary angle rotation was $-0.1 \pm 0.2°$, and for secondary angle rotation it was $0.1 \pm 0.2°$. The image-based orientation measurement error for primary angle rotation was $-0.1 \pm 1.3°$, and for secondary angle rotation it was $-1.3 \pm 0.3°$.
Conclusion The accelerometer provided better results than the built-in sensor and image-based tracking. The accelerometer sensor is small, inexpensive, covers the full rotation range of the C-arm, does not require line of sight, and can be easily installed to any mobile X-ray machine. Therefore, accelerometer tilt sensing is a very promising applicant for orientation angle tracking of C-arm fluoroscopes.

Keywords Accelerometer · C-arm · Tilt sensor · Angle measurement · Accuracy study · Brachytherapy

Introduction

X-ray fluoroscopy is arguably the most used surgical guidance modality today. For three-dimensional computation using fluoroscopic X-ray images, a method is needed that delivers a precise spatial description of the C-arm during its operation. There are several techniques that are able to measure such a spatial description. This measurement is often described as tracking, whereupon the spatial description of an object is always tracked relatively to another object. In C-arm fluoroscopy, the rotating arm's position is relatively described to a stationary object, e.g., the base of the mobile X-ray device, which is not moving during the operation. The C-arm's orientation can be tracked by optical, electromagnetic or image-based measurement systems. Built-in encoders, integrated into the C-arm, are another possible option for orientation measurement. All methods are well known in engineering to be used for position or orientation estimation, but there are several limitations that come along with their usage or when installing them in an operating room.

Highly regarded due to its reliable and precise position tracking are optical measurement systems [1]. Optical active

T. Wolff (✉) · M. Eblenkamp · E. Wintermantel
Technische Universität München, Munich, Germany
e-mail: thomas.wolff@mytum.de

A. Lasso · G. Fichtinger
Queen's University, Kingston, ON, Canada

Published online: 03 July 2013

or passive infrared systems operate by emitting and capturing electromagnetic radiation by light emitting diodes and charge-coupled device cameras. Active systems send out infrared light, whereas passive systems use reflective objects that send back infrared light, which is usually also emitted by the camera. These systems are generally laborious to install with an extra calibration step and expensive. Nevertheless, the most detaining drawback is that they require line of sight in between the tracking camera and the light emitting object, which is meant to be tracked [1]. This emerges to be difficult in a busy operating room where several devices are operated simultaneously and staff is required to move freely for operation.

Electromagnetic tracking systems are based on two major components. One is an electromagnetic field generator, which creates a pulsed magnetic field of know geometry. The second component is an electromagnetic field sensor that can be placed in surgical instruments for example [1]. Ferromagnetic materials like most metals can distort the electromagnetic field and therefore reduce tracking accuracy. The device that is most disruptive for the electromagnetic field within the operating room is the C-arm. If the X-ray source or the image intensifier is too close to the electromagnetic emitter, it can cause severe distortions [2]. Another difficulty arises from the maximum size for the magnetic field that can be generated by the system. The C-arm's rotation diameter is too large for available electromagnetic tracking systems.

Image-based orientation measurement uses a radio-opaque object, commonly referred to as fiducial, that is inserted into the imaging field [3]. After a C-arm image is acquired, the projection geometry of the fiducial is used to reconstruct the C-arm orientation. After image acquisition, different types of features within the fiducials must be segmented and a computation of the projection has to be calculated. This requires a post-processing step which eliminates the possibility of having real-time orientation data [3]. Furthermore, the fiducial requires valuable space in the imaging field that is needed during the intervention. It might even interfere with the intervention as it overlays with imaged anatomy and therefore might cause misinterpretation of the images.

Modern C-arms incorporate joint encoders. The joint encoding feature is usually realized by mechanical, optical, or electrical sensors. Built-in encoders are not considered standard equipment for C-arms. They are sometimes included when the system is motorized. These systems are more expensive than C-arms without motorization. Care facilities with lower budgets tend not to invest in motorized C-arms.

The immediate clinical driver for this work was prostate brachytherapy, which is one of the definitive treatment options for early stage localized prostate cancer. Brachytherapy aims to eliminate cancer with radiation by permanently implanting radioactive capsules, so called seeds, into the prostate [4]. Brachytherapy is predominantly performed with transrectal ultrasound (TRUS) guidance that provides adequate real-time visualization of the prostate but not of the implanted seeds. Despite significant efforts, localization of seeds directly from TRUS has not been clinically practical or robust. C-arm fluoroscopy is widely used for gross visual assessment of the implant, but it cannot show the prostate. Recently, reconstruction of implanted seeds from fluoroscopy has become possible in standard clinical settings, with average C-arm fluoroscopes [5,6]. For three-dimensional seed localization, multiple images are acquired at known relative orientation. In order to make brachytherapy seed reconstruction feasible with any mobile X-ray imaging device, an inexpensive and robust orientation measurement system is needed that is widely applicable, hence a retrofit system that is convenient to install and operate. The orientation measurement system must not interfere with brachytherapy workflow and must deliver the orientation information in real time, with an accuracy comparable to built-in encoders. In brachytherapy, due to collision with the patient, table and implant equipment, the C-arm rotates about the AP axis within a 30° rotational cone. It has been established that about 2 degree accuracy in rotational pose measurement of a C-arm is satisfactory for brachytherapy implant reconstruction [5,6].

C-arm angle measurement allows several other clinical applications, such as automatic alignment of the viewing angle of pre-procedural volumetric images with the current fluoroscopic view, or fused 3D display of left atrium over the live fluoroscopy image to serve as a roadmap during epicardial ablation procedures. These applications can tolerate up to a few degrees of error in C-arm angle measurement accuracy.

Preliminary experiments showed useful results sensing the rotation of a miniature C-arm model with an accelerometer used as a tilt sensor [7]. In this paper, we extend the work to a full-scale clinical C-arm with an improved calibration process and we evaluate the approach to recover C-arm orientation using an accelerometer in the context of prostate brachytherapy.

Materials and methods

Angle measurement with accelerometer

Innovative part of the system is the tri-axial accelerometer sensor. Basic idea is to use the accelerometer as a tilt sensor at static positions, which has not been done on a C-arm before. Grzeda et al. mounted an accelerometer on a miniature model of a C-arm that is able to simulate the rotational movement of such a mobile X-ray machine [7]. They collected tri-axial acceleration data for different static positions within a 30° rotational cone. In order to validate the angle readings of the

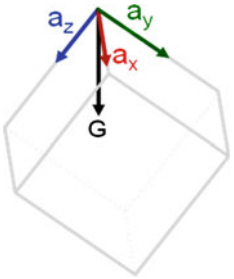

Fig. 1 Tri-axial accelerometer model under influence of gravity. Acceleration is distributed according to its direction among three orthogonal axes

accelerometer, they obtained ground truth poses with a digital webcam that tracked a checkerboard plate. The checkerboard projection images were used to calculate the ground truth pose of the C-arm model. Based on the promising results of these initial experiments, we improved the system using an accelerometer with higher resolution and we transferred the system to a real C-arm.

By means of the acceleration measurements, the orientation of the accelerometer and therefore the C-arm's orientation can be computed. Each axis of the accelerometer measures the influence of gravity (Fig. 1).

In a static position, only acceleration induced by gravity is applied to the tri-axial sensor. The manufacturer of the accelerometer specifies that the measurements a_x, a_y and a_z of all three axes are normalized to 1G. Calculating a desired angle in between an axis or a pair of axes with respect to the direction of gravitational force, which is always to the ground, is a matter of reformulating Eq 1.

$$1G = \sqrt{a_x^2 + a_y^2 + a_z^2} \tag{1}$$

A tri-axial micro-electro-mechanical system (MEMS) accelerometer was used in this work (1056-PhidgetSpatial 3/3/3, Phidgets Inc. Calgary, AB, Canada). The device measures acceleration in 3 axes up to 5 G. The measured value naturally incorporates the gravity vector, which is a force that induces acceleration to any object on earth toward ground. The three accelerometer axes are orthogonal, and each one returns the acceleration of one axis. At a standstill, each axis will measure in between ± 1.0 G depending on orientation. This reflects the effect of gravity. The output corresponding to each axis is a value proportional to the projection of the total acceleration along its direction. The accelerometer has a resolution of 230 µg which corresponds to a theoretical angular resolution of 0.2° considering the C-arm's radius and applying trigonometry. The PhidgetSpatial was directly connected to a computer via USB, and the data were acquired using the PLUS toolkit [8].

Three-way angle measurement

We used an optical tracking system to verify the measured C-arm angles. In addition, we calibrated the C-arm as in [3,9] and compared the C-arm angle measurement results with built-in encoder and image-based angle measurement. The integration of other tracking methods facilitates the comparison of accelerometer-based tracking with competing systems. Figure 2 illustrates the evaluation process of the accelerometer-based, the encoder-based, and the image-based orientation estimation. The optical measurement system is used as ground truth information. The difference between one orientation estimation modality and ground truth is the orientation angle error of the tracking method. Errors in the three orientations were computed and collected in an error statistics overview. This overview allows an accuracy analysis for all systems and a direct comparison in between the different tracking modalities.

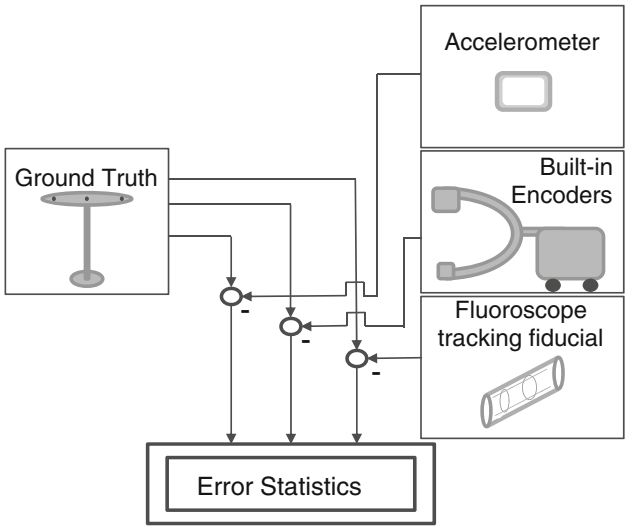

Fig. 2 Error computation of C-arm measurement methods. The error is the difference between tracked orientation and ground truth

C-arm

The mobile C-arm X-ray machine used in this work is an OEC 9800 manufactured by GE OEC Medical Systems, Salt Lake City, Utah, USA. The C-arm has motorized primary and secondary rotational motion axes. The definition of primary and secondary rotation axes are illustrated in Fig. 3. The primary and secondary position angles of the C-arm are measured by built-in sensors and displayed on the C-arm's screen. The image intensifier has a diameter of 12 in. featuring a central resolution at 1.5 line pairs per millimeter. In addition to its roller wheels, there are rotational and translational degrees of freedom allowing for proper positioning of the device around the patient. The center position of the C-arm is at 0° of the primary and secondary axis with the image intensifier in the upper position. The maximum rotation ranges of the primary and secondary rotation axis are 125° and 360°, respectively.

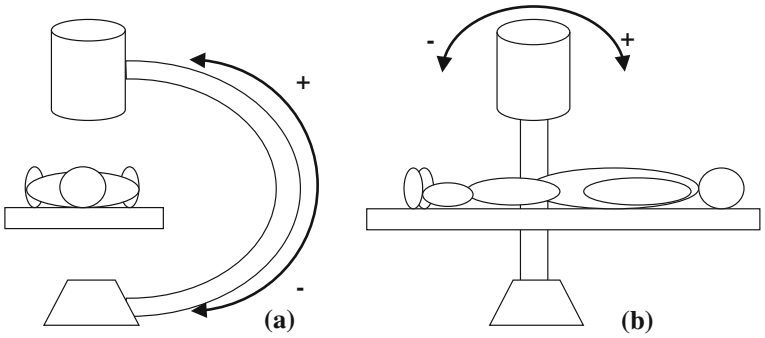

Fig. 3 Primary angle (**a**) and secondary angle (**b**) rotations of the C-arm

Fluoroscope tracking fiducial

Single-image-based fluoroscope tracking (FTRAC) is a method to measure the pose of the X-ray image with a fiducial [3,9,10]. We applied Jain's FTRAC device, which consists of a set of ellipses, lines, and points that can be identified in an X-ray image. The fiducial projection creates a unique 2D image from any direction. The unique projection image can be used to determine the pose of the fiducial pose during image acquisition, respectively, the C-arm's pose. The FTRAC system that was used in the experiments was a prototype provided from The Johns Hopkins University. The fiducial was mounted onto a stand with a holder that placed it stationary in the imaging field of the C-arm which rotated around it, by means of a software comprised in the system, the C-arm's pose can be calculated by determining transformations between the coordinate frames of the C-arm and the fiducial.

Ground truth pose

The most suitable measurement device for ground truth measurement is optical tracking. The system that was used as an optical sensor is an OptotrakCertus manufactured by Northern Digital Inc., Waterloo, ON, Canada. The OptotrakCertus system is an optical measurement device used to track the position of infrared light emitting diodes. The active infrared stylus tracking was used to detect landmarks on the C-arm. Landmarks are geometric bodies that are easily detectable by the stylus. Multiple landmarks distributed on the C-arm enable tracking of the C-arm's rotation. More specifically, the system enables active infrared stylus tip position tracking with a measurement accuracy of 0.1 mm. This resolution can be reformulated to a rotational angle accuracy of about 0.02°, considering the approximately 1,000-mm tracked landmark distance from the arm's rotation axis.

Calibration

In order to improve angle measurement results, a one-time calibration procedure is performed. The calibration workflow is illustrated in Fig. 4. First, the sensor is installed on

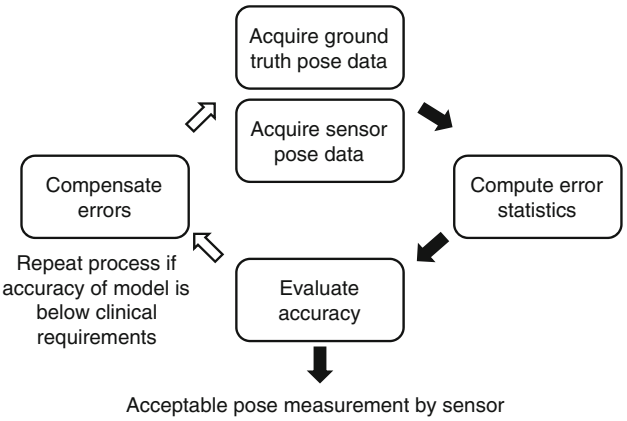

Fig. 4 Sensor calibration workflow

the C-arm. As it is not feasible to fix the FTRAC tracking fiducial in the field of view of the C-arm, a one-time calibration procedure is not possible for the image-based method. The C-arm is rotated into an initial position. In this position, two measurements are recorded: the orientation data provided by the sensor (accelerometer or built-in encoder) and the ground truth orientation data. Afterward, the C-arm is rotated along one of the axes with a pre-defined angle interval. In this second position, sensor data and ground truth orientation data are recorded again. The records are taken for all orientations along the maximum rotation range of the C-arm at pre-defined intervals. After one axis is completed, the second rotation axis of the C-arm is measured in the same way. A calibration function is constructed by polynomial fitting of the raw accelerometer angle measurements verses the ground truth angles. The calibrated angle values are computed by transforming the sensor-provided values by the calibration function. The calibration process is only needed once after the installation of the sensor. It does not have to be repeated as long as the sensor is not removed from the C-arm.

Data acquisition

C-arm orientation was measured in a repetitive multimodality data acquisition experiment that is illustrated in Fig. 5. The C-arm orientation was tracked for both rotation

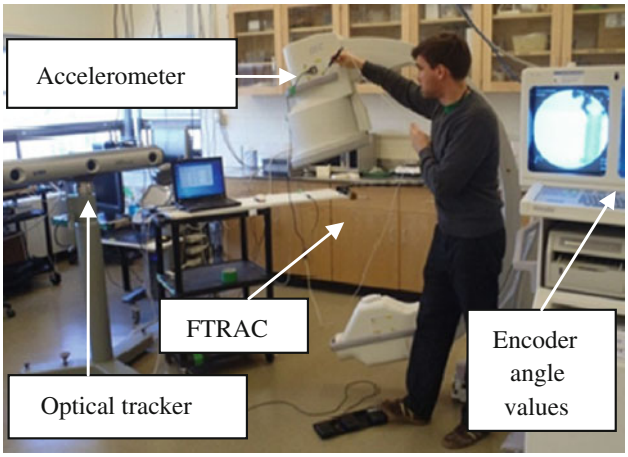

Fig. 5 C-arm rotation angles measured by optical tracker, accelerometer, imaging the FTRAC fiducial, and by reading the values provided by the built-in encoder

modes that are referred to as primary and secondary rotation angles. The rotation range was chosen to cover the operating distance of the C-arm during prostate brachytherapy procedure. Therefore, rotation motion range for both rotational axes was set to 30°, which complies with a rotation of ±15° around the center position of the C-arm. The measurement started in the negative rotation range and the interval in between two measurements was set to 1°. The FTRAC fiducial was placed stationary in the center of the imaging field by a holder, and then, the C-arm was moved into an initial position. The C-arm orientation was first measured with the optical measurement system by touching fixed landmarks on the C-arm with the tracked stylus. A landmark on the stationary base of the C-arm served as reference. All other landmarks were located on the rotating parts of the C-arm. The orientation ground truth measurement for each position of the C-arm started with the measurement of the fixed base landmark. All landmarks that changed orientation due to rotation were described relatively to the stationary reference. Subsequent to the recording of ground truth orientation a fluoroscopic image of the FTRAC fiducial was acquired. The X-ray images were post-processed after all data acquisition was completed to obtain orientation information. After the X-ray image acquisition, the accelerometer reading was recorded. The mean of the accelerometer reading with a sampling rate of 8 ms over 1 s was calculated. The built-in encoder orientation value displayed on the C-arm screen was also recorded. Subsequently to the data acquisition of the initial position, the C-arm was rotated to the next measurement position. All four orientation estimation modalities were carried out for 31 positions in the rotation range of a brachytherapy intervention. This was done for both primary and secondary rotation modes of the C-arm.

Results

The results in this section represent orientation angle estimation data recorded by four tracking methods—optical tracking (ground truth), accelerometer orientation angle estimation, built-in encoder orientation angle estimation, and image-based orientation angle estimation with the FTRAC device. The values represent the orientation angle information of the C-arm for 31 positions (−15° to +15°) on the primary and secondary angle rotation axis. 0° corresponds to the C-arm's vertical position.

The initial orientation angle estimations without calibration for all tracking methods are plotted for primary and secondary angle rotations in Fig. 6. The graphs show the tracking methods estimated orientation angle values plotted against ground truth. The built-in encoder orientation estimation is very close to ground truth. The accelerometer orientation estimation follows ground truth with a constant offset for primary and secondary angle rotation. The image-based orientation estimation has a different slope for both rotation modes.

Figure 7 shows the orientation angle results after calibration against ground truth.

The calibration brings the tracked orientation angle data closer to ground truth values. Calibration is not applicable to image-based tracking; therefore, uncalibrated results are shown for comparison. The orientation angle errors for each position of the 31 C-arm positions of each tracking method were calculated. The orientation angle errors of accelerometer, built-in encoder, and image-based tracking estimation for both the primary and secondary angle rotations are shown in Fig. 8.

The mean and standard deviation of the angle error were calculated for all tracking methods. This was done for primary angle rotation as well as for secondary angle rotation. The initial angle errors before calibration were compared with the angle errors after calibration. The results for primary and secondary angle rotations are shown in Tables 1 and 2.

The angle measurement error histograms shown in Figs. 9 and 10 further illustrate the outcome of the calibration procedure applied to the tracking methods.

In summary, accuracy of orientation angle estimation with the accelerometer and the built-in encoders were both very good. Precision of the accelerometer-based angle estimation was much better compared to the built-in encoders, as demonstrated by the narrower histogram shape and lower standard deviation value. The FTRAC-based estimation method provided similar results as obtained by uncalibrated accelerometer and built-in encoder. However, compared to FTRAC, the other methods had considerable better accuracy and precision after calibration.

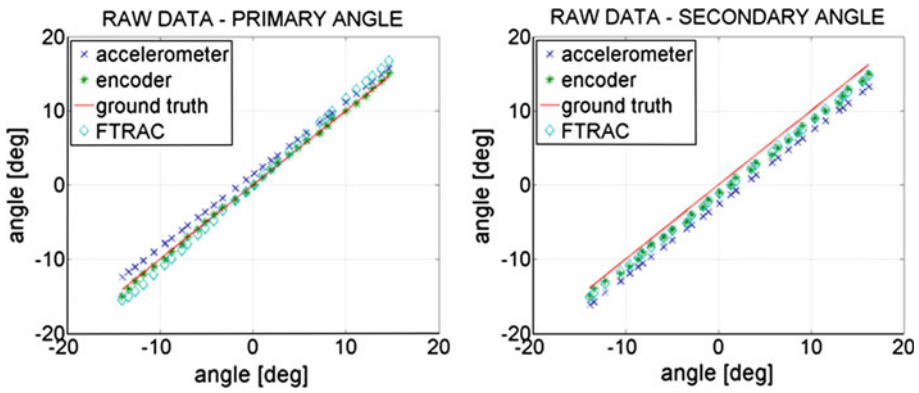

Fig. 6 Initial orientation angle estimation of accelerometer, built-in encoder, and image-based tracking for the primary angle (*left*) and secondary angle (*right*)

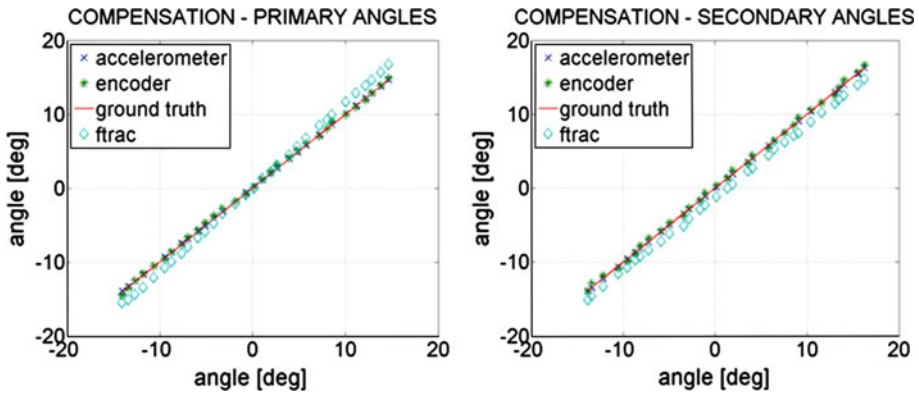

Fig. 7 Orientation angle estimation of the accelerometer, built-in encoder, and image-based tracking (FTRAC) after calibration, for the primary angle (*left*) and secondary angle (*right*). Calibration is not applicable to image-based tracking; therefore, uncalibrated results are shown for FTRAC

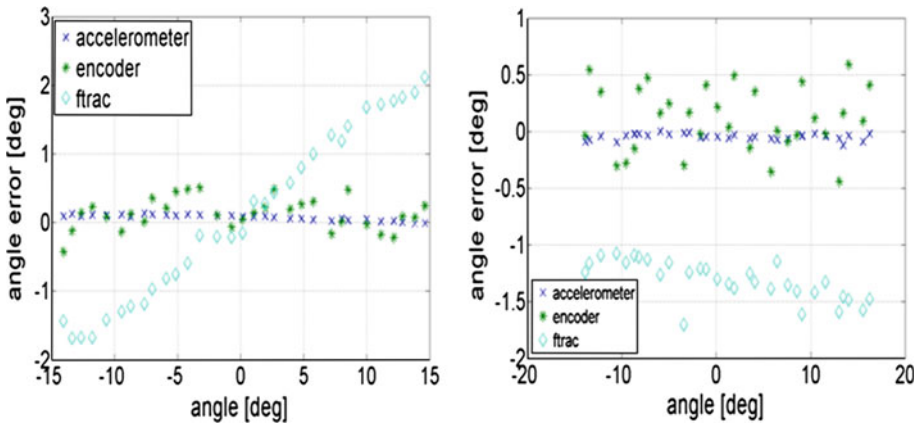

Fig. 8 Orientation angle errors of the accelerometer, built-in encoder, and image-based tracking, for the primary angle (*left*) and secondary angle (*right*). Image-based tracking (FTRAC) results are without applying calibration

Table 1 Mean angle errors for primary angle rotation of accelerometer, mechanical encoder, and image-based orientation angle estimation

Primary angle rotation	Orientation angle error (initial)	Orientation angle error (after calibration)
Accelerometer	$1.3 \pm 0.1°$	$-0.1 \pm 0.0°$
Built-in encoder	$-0.2 \pm 0.3°$	$-0.1 \pm 0.2°$
FTRAC	$-0.1 \pm 1.3°$	N/A

Table 2 Mean angle errors for secondary angle rotation of accelerometer, mechanical encoder, and image-based orientation angle estimation

Secondary angle rotation	Orientation angle error (initial)	Orientation angle error (after calibration)
Accelerometer	$-2.6 \pm 0.2°$	$0.1 \pm 0.0°$
Built-in encoder	$-1.4 \pm 0.3°$	$0.1 \pm 0.2°$
FTRAC	$-1.3 \pm 0.3°$	N/A

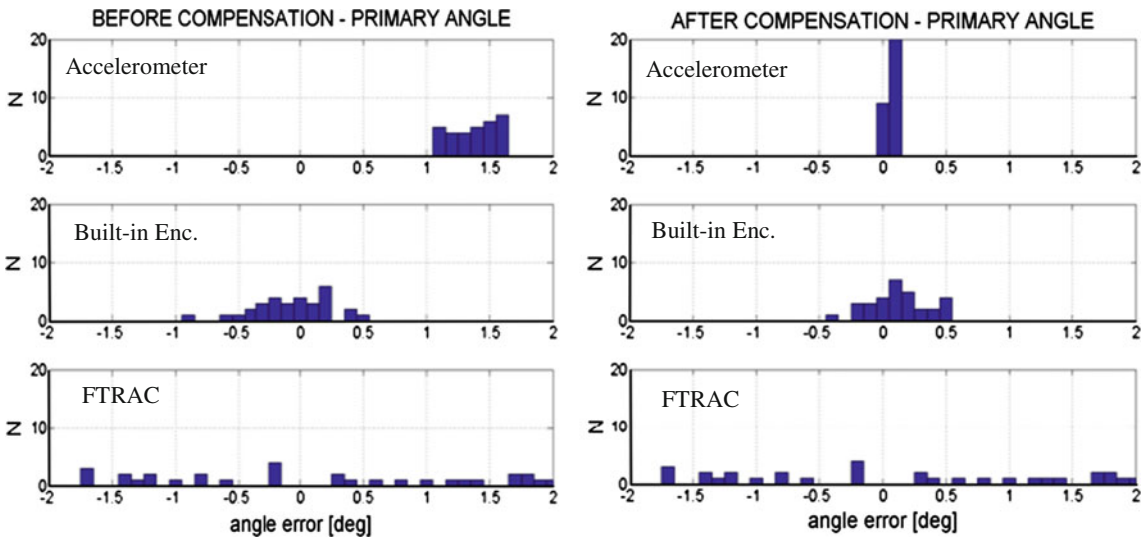

Fig. 9 Histograms showing the angle error distribution for primary angle rotation before calibration (*left*) and after (*right*), with accelerometer (*top row*), built-in encoder (*middle row*), and FTRAC (*bottom row*). The histogram bin size is 0.1°

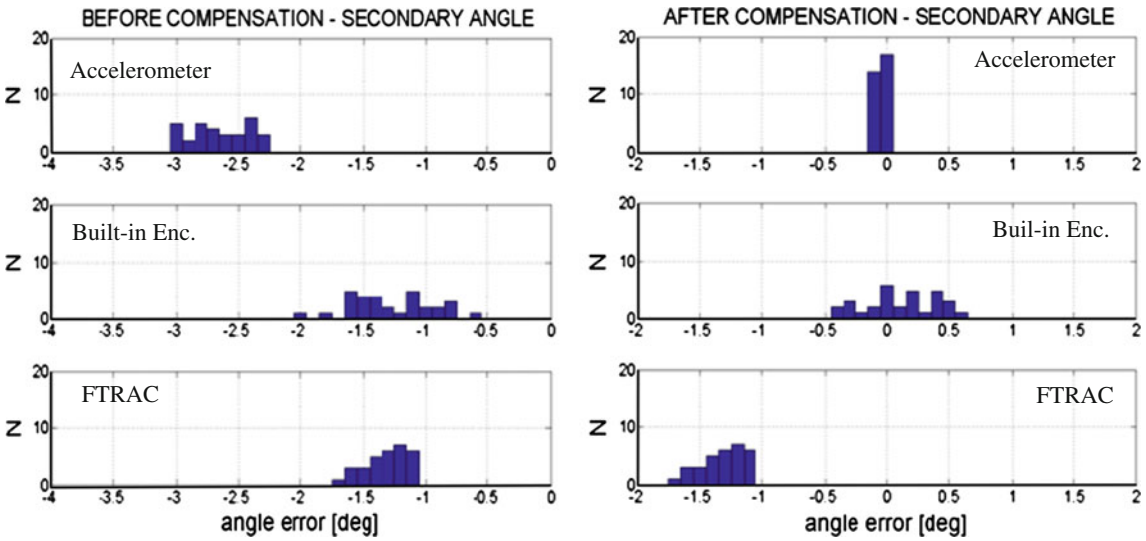

Fig. 10 Angle error distribution for secondary angle rotation before calibration (*left*) and after (*right*)

Discussion

The accelerometer proved to be able to provide sufficiently accurate C-arm orientation angle estimation for both the primary and secondary rotations. The initial orientation estimation of the accelerometer without calibration delivered useful results. This was probably the outcome of a deliberate setup that paid attention to optimal alignment of the tri-axial acceleration sensor when mounted onto the C-arm. The accelerometer axes are supposed to be aligned with both C-arm rotation axes and the direction of gravity. Since such an alignment is laborious and subjective, we propose and conducted a software-based calibration process that prevents user errors during setup. The calibration procedure makes up for any misalignments of the acceleration sensor. The accelerometer can be fixed in any position and orientation on the moving part of the C-arm. After calibration, it will deliver accurate readings. Mounting the sensor becomes an easy installation step when using a calibration method afterward. The built-in encoder angle estimation showed also accurate results regarding the C-arm's orientation recovery. The calibration process was able to further improve the results. However, in the experiments, a position of the C-arm was always approached from the same direction. This reduced the mechanical effect of backlash of the C-arm. During common operation of the machine, the mechanical tolerance was occasionally noticeable. This might affect the accuracy of the built-in encoder orientation estimation and increase the orientation estimation mean error of the system. FTRAC-based fluoroscope tracking did not deliver reproducible results in

the orientation angle acquisition evaluation. The problem was that the calibration process for the FTRAC-based tracking method requires the same relative position in between the FTRAC fiducial and the C-arm for each application. In order to accomplish this task, the FTRAC fiducial had to be positioned near the center position of the imaging field of the C-arm, with a specified orientation. The positioning was a laborious trial and error method, especially when trying to cover the edges of the motion range for the brachytherapy application motion range of 30°. Although the positioning was carried out very carefully, sometimes the acquired X-ray images did not contain all radio-opaque features of the fiducial. Hence, the image segmentation necessary for orientation estimation could not be achieved. It was impossible to set the system up in the same way at different times. Therefore, the FTRAC-based angle estimation showed big differences in the results for this experimental setup, which made repeatable results unfeasible.

The accelerometer performance orientation estimation was evaluated in static positions only, as during C-arm motion, the sensor measurement includes the acceleration caused by the rotational motion. For a preliminary evaluation of this error, we recorded angle data computed by accelerometer and optical tracker during C-arm rotation. We used the optical tracker measurement as ground truth and found that in 95 % of the time the accelerometer-based data (after a simple moving average filtering) had well below 1° error. This error is already acceptable for several use cases. To fulfill the requirements of more demanding applications—such as cone-beam reconstruction—the angle estimation error can be further reduced by introducing additional sensors, such as gyroscopes and applying sensor fusion algorithm to suppress the effect of the motion-induced acceleration.

Conclusion and future work

An accelerometer-based method to recover C-arm orientation was compared with other tracking modalities and evaluated in an experimental setup that simulated prostate brachytherapy seed reconstruction. It was shown that accelerometer orientation estimation is an eligible candidate for C-arm orientation angle tracking whenever built-in encoders are not available or not accurate enough. The accelerometer orientation angle readings presented similar or better accuracy and better precision than the built-in encoder of the C-arm. The accelerometer also provided better angle accuracy and precision than the FTRAC-based fluoroscope tracking system. The low investment costs and the ability to equip any C-arm model qualify the accelerometer as a low-cost retrofit alternative for C-arm orientation measurement. The accelerometer sensor is widely applicable as it does not interfere with any other systems in the operating room. The accelerometer is convenient to use owing to its simple installation and operation. The reading of the accelerometer sensor is available in real time.

Accelerometer-based C-arm angle measurement was found to be convenient and accurate enough method for prostate brachytherapy seed reconstruction and for basic image viewing angle synchronization and roadmapping applications. Future research will focus on orientation measurement during C-arm motion by using angular rate sensors in addition to accelerometers.

Acknowledgments This work was supported through the Applied Cancer Research Unit program of Cancer Care Ontario with funds provided by the Ontario Ministry of Health and Long-Term Care. Gabor Fichtinger was funded as a Cancer Ontario Research Chair. The authors thank Yashar Madjidi for the fabrication of the C-arm calibration phantom.

Conflict of interest Thomas Wolff, Andras Lasso, Markus Eblenkamp, Erich Wintermantel and Gabor Fichtinger declare that they have no conflict of interest.

References

1. Cleary K, Peters TM (2010) Image-guided interventions: technology review and clinical applications. Ann Rev Biomed Eng 12:119–142
2. Wegner I, Teber D, Hadaschik B, Pahernik S, Hohenfellner M, Meinzer H-P, Huber J (2012) Pitfalls of electromagnetic tracking in clinical routine using multiple or adjacent sensors. Int J Med Robotics Comput Assist Surg. 4 Apr, 2012. doi:10.1002/rcs.1431 [Epub ahead of print]
3. Jain AK, Mustafa T, Zhou Y, Burdette C, Chirikjian GS, Fichtinger G (2005) FTRAC—a robust fluoroscope tracking fiducial. Med Phys 32(10):3185–3198
4. Wallner K, Blasko JC, Dattoli M (2001) Prostate brachytherapy made complicated. SmartMedicine Press, Seattle
5. Dehghan E, Moradi M, Wen X, French D, Lobo J, Morris WJ, Salcudean SE, Fichtinger G (2011) Prostate implant reconstruction from C-arm images with motion-compensated tomosynthesis. Med. Phys. 38(10):5290–5302
6. Lee J, Labat C, Jain AK, Song DY, Burdette EC, Fichtinger G, Prince JL (2011) REDMAPS: reduced-dimensionality matching for prostate brachytherapy seed reconstruction. IEEE Trans Med Imaging 30:38–45
7. Grzeda V, Fichtinger G (2010) C-arm rotation encoding with accelerometers. Int J Comput Assist Radiol Surg 5(4):385–391
8. Lasso A, Heffter T, Pinter C, Ungi T, Chen TK, Boucharin A, Fichtinger G (2001) PLUS: an open-source toolkit for developing ultrasound-guided intervention systems. In: Proceedings 4th NCIGT and NIH, Image Guided Therapy Workshop, Arlington, VA. 4, pp 103
9. Chintalapani G, Jain AK, Burkhardt DH, Prince JL, Fichtinger G (2008) CTREC: C-arm tracking and reconstruction using elliptic curves. In: IEEE computer society conference on computer vision and pattern recognition workshops, cvprw, pp 1–7
10. Yao J, Taylor RH, Goldberg RP, Kumar R, Bzostek A, Van Vorhis R, Kazanzides P, Gueziec A (2000) A C-arm fluoroscopy-guided progressive cut refinement strategy using a surgical robot. Comput Aided Surg 5(6):373–390